CORRELATIONS BY THE ENTRAINMENT THEORY OF THERMODYNAMIC EFFECTS FOR DEVELOPED CAVITATION IN VENTURIS AND COMPARISONS WITH OGIVE DATA

M. L. Billet, J. W. Holl, and D. S. Weir

Technical Memorandum
File No. TM 75-291
December 11, 1975
Contract No. N00017-73-C-1418

Copy No. 9

The Pennsylvania State University
Institute for Science and Engineering
APPLIED RESEARCH LABORATORY
Post Office Box 30
State College, PA 16801

NAVY DEPARTMENT

NAVAL SEA SYSTEMS COMMAND

SECURITY CLASSIFICATION OF THIS PAGE (When Data Entered)

REPORT DOCUMENTATION PAGE

READ INSTRUCTIONS BEFORE COMPLETING FORM

1. REPORT NUMBER
TM-75-291

2. GOVT ACCESSION NO.

3. RECIPIENT'S CATALOG NUMBER

4. TITLE (and Subtitle)
CORRELATIONS BY THE ENTRAINMENT THEORY OF THERMODYNAMIC EFFECTS FOR DEVELOPED CAVITATION IN VENTURIS AND COMPARISONS WITH OGIVE DATA.

5. TYPE OF REPORT & PERIOD COVERED
Technical Memo[redacted]

6. PERFORMING ORG. REPORT NUMBER

7. AUTHOR(s)
M. L. Billet, J. W. Holl[redacted] D. S. Weir

8. CONTRACT OR GRANT NUMBER(s)
NGL-39-009-001

9. PERFORMING ORGANIZATION NAME AND ADDRESS
Applied Research Laboratory
P. O. Box 30
State College, PA 16801

10. PROGRAM ELEMENT, PROJECT, TASK AREA & WORK UNIT NUMBERS
N00017-73-C-1418

11. CONTROLLING OFFICE NAME AND ADDRESS (Joint sponsorship)
National Aeronautics and Space Administration
Cleveland, OH 44135 and
Naval Sea Systems Command, Washington, DC 20362

12. REPORT DATE
11 Dec[redacted]975

13. NUMBER OF PAGES
41

14. MONITORING AGENCY NAME & ADDRESS (if different from Controlling Office)

15. SECURITY CLASS. (of this report)
UNCLASSIFIED

15a. DECLASSIFICATION DOWNGRADING SCHEDULE

16. DISTRIBUTION STATEMENT (of this Report)
Approved for public release. Distribution unlimited.
Per NAVSEA - May 3, 1976.

17. DISTRIBUTION STATEMENT (of the abstract entered in Block 20, if different from Report)

18. SUPPLEMENTARY NOTES

19. KEY WORDS (Continue on reverse side if necessary and identify by block number)
Cavitation, Venturis, Ogives, Thermodynamic Effects, Temperature Depression Correlations

20. ABSTRACT (Continue on reverse side if necessary and identify by block number)

A semi-empirical entrainment theory was employed to correlate the measured temperature depression, ΔT, in a developed cavity for a venturi. This theory correlates ΔT in terms of the dimensionless numbers of Nusselt, Reynolds, Froude, Weber and Péclet, and dimensionless cavity length, L/D. These correlations are then compared with similar correlations for zero and quarter caliber ogives. In addition, cavitation number data for both limited and developed cavitation in venturis are presented.

DD FORM 1 JAN 73 1473 EDITION OF 1 NOV 65 IS OBSOLETE

UNCLASSIFIED
SECURITY CLASSIFICATION OF THIS PAGE (When Data Entered)

Abstract: A semi-empirical entrainment theory was employed to correlate the measured temperature depression, ΔT, in a developed cavity for a venturi. This theory correlates ΔT in terms of the dimensionless numbers of Nusselt, Reynolds, Froude, Weber and Péclét, and dimensionless cavity length, L/D. These correlations are then compared with similar correlations for zero and quarter caliber ogives. In addition, cavitation number data for both limited and developed cavitation in venturis are presented.

Table of Contents

	page
Abstract	1
Table of Contents	2
List of Tables	3
List of Figures	3
Nomenclature	4
I. Introduction	5
II. Empirical Equations for C_A, C_Q, Nu and ΔT	8
III. Experimental Results for the Venturis	9
A. Description of the Experiments	9
B. Determination of Cavitation Number	10
C. Determination of the Flow Coefficient	11
D. Determination of Cavity Geometry	13
IV. Application of the Entrainment Theory	13
V. Conclusions	15
VI. Acknowledgments	16
VII. References	16
Tables	19
Figures	31

List of Tables

Table		Page
I	Tabulation of Experimental Data for the Venturis . . .	19
II	Constants and Exponents for Entrainment Theory - First Correlation	24
III	Constants and Exponents for Entrainment Theory - Second Correlation	25
IV	Constants and Exponents for C_A Correlation	26
V	Comparison of Measured ΔT with Calculated ΔT for the Venturis	27
VI	ΔT Correlations for Constant Fluid Properties	30

List of Figures

Figure		Page
1	Photograph of the Ultra-High Speed Cavitation Tunnel	31
2	Photograph of the Venturis: A. 0.7 Scale Venturi (0.975-inch Diameter) and B. Full Scale Venturi (1.378-inch Diameter) with Air Injection Ring	32
3	Sketch of the Full Scale Venturi	33
4	Limited Cavitation Number Versus Reynolds Number for Venturis	34
5	Cavitation Number for Developed Cavitation on 0.7 Scale Venturi	35
6	Cavitation Number for Developed Cavitation on Full Scale Venturi	36
7	Flow Coefficient for 0.7 Scale Venturi	37
8	Flow Coefficient for Full Scale Venturi	38
9	Area Coefficient for the Venturis	39
10	Dimensionless Minimum Cavity Diameter for the Venturis	40
11	Sketch of the Ogives and Description of Test Conditions	41

Nomenclature

A_w - cavity surface area

B - ratio of vapor volume to liquid volume involved in sustaining a natural cavity

C_A - area coefficient $\equiv A_w/D^2$

C_p - specific heat of liquid

C_Q - flow coefficient $\equiv Q/V_\infty D^2$

D - model diameter

D_m - minimum cavity diameter

Fr - Froude number $\equiv V_\infty/\sqrt{gD}$

g - acceleration of gravity

h - film coefficient $\equiv \dot{q}/A_w \Delta T$

k - thermal conductivity of liquid

L - cavity length

Nu - Nusselt number $\equiv hD/k$

P_c - cavity pressure

Pe - Péclét number $\equiv V_\infty D/\alpha$

Pr - Prandtl number $\equiv \nu/\alpha$

P_v - vapor pressure

P_∞ - free stream pressure

$\dot{q}$ - heat transfer rate

Q - volume flowrate of vapor in cavity

Re - Reynolds number $\equiv V_\infty D/\nu$

T_c - cavity temperature

T_∞ - free stream temperature

ΔT - temperature depression* $\equiv T_\infty - T_c$

V_∞ - free stream velocity

We - Weber number $\equiv V_\infty \sqrt{D}/\sqrt{S/\rho}$

α - thermal diffusivity of liquid

λ - latent heat of vaporization

ν - kinematic viscosity of liquid

ρ_L - mass density of liquid

ρ_v - mass density of vapor

σ - cavitation number

S - surface tension

* All experimental values of ΔT are maximum values obtained from axial surveys of the cavity.

I. Introduction

Cavitation is an important consideration in the design and analysis of liquid handling pumps. Limited cavitation occurs whenever the local pressure is reduced to some critical value. A further reduction in pressure results in developed cavitation. In this flow regime, it is difficult to predict the net positive suction head (NPSH) required for the satisfactory performance of a pump. The NPSH requirements are determined by the combined effects of cavitation, fluid properties, pump geometry and pump operating point.

The determination of the cavity pressure is of primary importance in understanding the influence of developed cavitation on pump performance. In most cases, the designer assumes that the cavity pressure is equal to the vapor pressure at the bulk temperature of the liquid. This estimate is quite good in the absence of noncondensable gases when P_V and dP_V/dT are both small. This occurs at states significantly below the critical temperature, for example water at room temperature, but for many fluids such as liquid metals and cryogens the operating temperature can be such that P_V and dP_V/dT are both large. In these cases, the assumption that the cavity pressure is equal to the vapor pressure corresponding to the bulk temperature of the liquid can lead to very large errors.

A continuous vaporization process which is dependent upon heat transfer at the liquid-vapor interface is required to sustain a developed cavity in a pump. As a result of vaporization, the cavity temperature is less than the inlet bulk liquid temperature so that the cavity vapor pressure is less than the vapor pressure corresponding to the inlet bulk liquid temperature. This phenomenon is called the thermodynamic effect and is dependent on fluid properties, velocity, size and geometry. The thermodynamic effect is important because the NPSH required to produce a given cavity volume will decrease as the temperature depression at the cavity increases.

Stahl and Stepanoff [1]* were the first to analyze the thermodynamic effect for developed cavitation with particular emphasis on pump applications. They formulated the B factor method which is quasi-static in nature. Fisher [2], Jacobs [3], and Acosta and Hollander [4] also considered the B factor method and its application.

The equation for predicting the temperature depression (ΔT) from the B factor method is

$$\Delta T = B \frac{\rho_V}{\rho_L} \cdot \frac{\lambda}{C_P} \tag{1}$$

---

* Numbers in brackets refer to documents in list of references.

where the factor B is defined as the ratio of vapor volume to liquid volume involved in the vaporization process. However, the primary practical problem which a designer encounters in attempting to use Equation (1) is the calculation of B.

In order to make the B factor method more useful as a data correlation method, Gelder et al. [5] and Moore and Ruggeri [6] extended it in a semi-empirical manner. They expressed the B factor in terms of dimensionless ratios

$$B = B_R \left\{\frac{V_\infty}{V_{\infty_R}}\right\}^{N_1} \left\{\frac{D}{D_R}\right\}^{N_2} \left\{\frac{L/D}{(L/D)_R}\right\}^{N_3} \left\{\frac{\alpha}{\alpha_R}\right\}^{N_4} \qquad (2)$$

and then determined the exponents empirically. The subscript R employed in Equation (2) indicates a reference value. Hord et al. [7, 8, 9] have further extended this approach by including other factors such as kinematic viscosity in Equation (2). Finally, Hord [10] has applied the correlation to pumps.

The entrainment theory was developed as an alternate to the B factor method for predicting the thermodynamic effect. It is a dynamical approach based on an energy balance for the cavity. It is semi-empirical like the B factor method but has the advantage of expressing the temperature depression in terms of basic physical quantities. The principal theoretical and experimental aspects of this theory are presented in Holl et al. [11] and Weir [12].

From the entrainment theory, the temperature depression (ΔT) is given by

$$\Delta T = \frac{C_Q}{C_A} \cdot \frac{Pe}{Nu} \cdot \frac{\rho_v}{\rho_L} \cdot \frac{\lambda}{C_p} \quad . \qquad (3)$$

The Péclét number and fluid property terms are known from the free stream conditions (T_∞ and V_∞) and the characteristic model dimension (D). However, C_A, C_Q and Nu are characteristic of the cavity flow and are to be determined empirically.

Extensive temperature depression data correlated by means of the entrainment theory have been reported for ogive nosed bodies [11] [12]. In addition, temperature depression data correlated by means of the B factor method have been reported for venturis [6] [7]. It was decided that it would be desirable to compare the venturi and ogive data when correlated by the entrainment theory. In order to accomplish this goal, it was necessary to experimentally determine the area coefficient (C_A) and flow coefficient (C_Q) for the venturis. These were then employed in Equation (3) to determine the Nusselt number by using the temperature depression data of Moore and Ruggeri [6] and Hord, et al. [7]. The ΔT data for the venturis were obtained in Freon 114, hydrogen and nitrogen whereas the ogive ΔT data were obtained in Freon 113 and water.

In addition to the aforementioned correlations of ΔT, cavitation number data for both limited and developed cavitation in venturis are also presented in this report.

II. Empirical Equations for C_A, C_Q, Nu and ΔT

In order to determine an equation which correlates ΔT data by means of the entrainment theory, i.e. Equation (3), it is necessary to determine empirical equations for C_A, C_Q and Nu in terms of pertinent physical parameters. An examination of the problem led to the following general forms for C_A, C_Q and Nu

$$C_A = C_1 \{L/D\}^a \tag{4}$$

$$C_Q = C_2 \, Re^b \, Fr^c \, We^d \, \{L/D\}^e \tag{5}$$

$$Nu = C_3 \, Re^f \, Fr^g \, We^h \, Pr^i \, \{L/D\}^j \tag{6}$$

As will be seen in subsequent sections, two combinations of terms were tried for C_Q and Nu. The first correlation refers to that correlation in which Weber number was not considered i.e. d=h=0. Whereas, the second correlation refers to that correlation in which Froude number was eliminated i.e. c=g=0.

Employing Equations (4) - (6) in Equation (3) yields the general empirical form for the temperature depression as

$$\Delta T = C_4 (L/D)^k \, Re^\ell \, Fr^m \, We^n \, Pr^p \, Pe \, \frac{\rho_v}{\rho_L} \frac{\lambda}{C_p} \tag{7}$$

The unknown constants for all of the correlations were determined by a modified least-squares approximation technique. Taking the logarithm reduces the equation to linear form. Then, as outlined by Becket and Hunt [13], minimizing the sum of the squares of the difference between the logarithm of the measured data and the correlative expression yields a set of simultaneous equations which can be solved for the unknown constants. Details concerning the application of this modified least square approximation technique to the entrainment theory are given by Weir [12].

III. Experimental Results for the Venturis

A. Description of the Experiments

The experiments were conducted in water near room temperature with two venturis test sections in the 1.5 inch ultra-high speed cavitation tunnel located in the Garfield Thomas Water Tunnel building of the Applied Research Laboratory at The Pennsylvania State University. A photograph of the facility is shown in Figure 1 and a detailed description of the facility and supporting equipment is given in Reference [14]. The facility is designed to permit large variations in velocity, pressure, and temperature for various liquids. The maximum operating conditions for these parameters is 300 fps, 1200 psia, and 300 °F.

The internal contours of the two geometrically similar venturi test sections are the same as those employed by NASA [6, 7]. The minimum internal diameter is 1.378 inches and 0.975 inches for the full scale and 0.7 scale venturi, respectively. A photograph of the venturis is shown in Figure 2 and a detailed sketch of the full scale venturi is shown in Figure 3. (Details of the two venturis are given in ARL Drawings SKD 70533 and SKD 70534.)

The venturi test sections are 3 inches longer than the standard test sections for the 1.5 inch cavitation tunnel. Therefore, it was necessary to construct a 3 inch cylindrical section for the lower leg of the facility and extensions for the four bars supporting the test section in the upper leg. (Details concerning these additional parts for the facility are given in ARL Drawing SKR 70532.)

The venturis were instrumented with a pressure port slightly upstream of the throat to measure the incoming velocity and four pressure ports downstream of the throat to measure the cavity pressure. Gas injection ports for forming ventilated cavities with nitrogen gas were distributed tangentially around the test section, and a manifold which fit over the exterior of the test section distributed gas to the injection ports. (This manifold is shown in the photograph of Figure 2.) In addition, two probes were installed downstream of the throat to determine the cavity thickness for use in the determination of C_A. The locations of the pressure ports, gas injection ports, and probes are shown in Figure 3 for the full scale venturi.

The following tests were performed with the two venturis:

1. Determination of Cavitation Number
   The cavitation number (σ) for developed cavitation was determined as a function of L/D for ventilated and natural cavities. For limited cavitation, σ was determined as a function of velocity.

2. Determination of the Flow Coefficient
   The flow coefficient (C_Q) was determined as a function of L/D, velocity and venturi diameter for ventilated cavities.

3. Determination of Cavity Geometry
   The area coefficient (C_A) and dimensionless cavity diameter (D_m/D) were determined as a function of dimensionless cavity length (L/D) for natural cavities.

The experimental data for the venturis are tabulated in Table I.

B. Determination of Cavitation Number

The cavitation number (σ) is defined as

$$\sigma = \frac{P_\infty - P}{1/2\rho V_\infty^{\,2}} \tag{8}$$

where P_∞, ρ, and V_∞ are the pressure at infinity, liquid mass density and velocity at infinity, respectively. The quantity P is an appropriate measure of the cavity pressure. For developed cavitation, this pressure is

$$P = P_c \tag{9}$$

where P_c is the measured cavity pressure whereas for limited cavitation it is

$$P = P_v \tag{10}$$

where P_v is the vapor pressure corresponding to the bulk temperature of the liquid.

For the venturis the reference pressure (P_∞) and velocity (V_∞) were measured in the section shown in Figure 3. The various pressures were measured by Pace variable reluctance transducers.

As is customary at the Garfield Thomas Water Tunnel, desinent cavitation was employed as the experimental definition of limited cavitation. The desinent cavitation number for the venturis is shown as a function of Reynolds number in Figure 4. It is seen that the desinent cavitation number for water compares favorably with the minimum pressure coefficient. However, the water results are consistantly higher than the experimental results for Freon 114 [15] and liquid hydrogen [16]. Gas effects on water and surface tension effects in liquid hydrogen [16] may cause trends of this type.

The cavitation number (σ) for developed ventilated and natural cavitation on the venturis is shown as a function of dimensionless cavity length (L/D) in Figures 5 and 6. These graphs show that σ is independent of L/D and that a value of σ equal to 2.32 can be utilized to represent all of the data for natural and ventilated cavities. This compares to a constant cavitation number of 2.47 from earlier tests by Moore and Ruggeri [6] and Hord et al. [7].

Investigators of axisymmetric bodies, see for example References [12], [17] and [18], have shown that the cavitation number is a single valued function of dimensionless cavity length. However, the venturi data in Figures 5 and 6 do not display this characteristic. As shown by Weir [19], blockage effects on ogive nosed bodies are such that as the blockage increases, the cavitation number tends to become independent of L/D. Perhaps the constant cavitation number characteristic of the venturi is due to a similar effect.

C. Determination of the Flow Coefficient

It is well known that there are many similarities between the characteristics of natural and ventilated cavities for the same value of dimensionless cavity length. (This applies only when the ventilated cavity operates in the reentrant jet regime [20].) The German hydrodynamicist H. Reichardt [18] was apparently the first to demonstrate this characteristic by showing that the drag coefficient for an axially symmetric body was the same for both natural and ventilated cavities provided the cavitation number based on cavity pressure was the same for both flow states. Billet [21] has shown that the geometric characteristics of natural and ventilated cavities on ogives are the same when the cavitation number is the same.

Early in the development of the entrainment theory for correlating temperature depression data it was felt that the aforementioned similarity principle would be applicable to the volume flowrate of gas in the cavity. Thus it was assumed that the characteristics of the flow coefficient for the vapor flow in the cavity would be approximated by the flow coefficient for a ventilated cavity having the same geometrical characteristics. Furthermore, it was decided to minimize the diffusion of gas at the cavity wall and thereby produce a value of C_Q which was based on the entire volume flowrate required to sustain a cavity of a given size. Billet [21] was the first to apply the similarity concept to the entrainment theory. Subsequently this work was improved and is reported in References [11], [12], [20] and [22].

The diffusion of air across the cavity wall was minimized by maintaining the air pressure in the cavity at the saturation pressure (P_{G-S}) of the dissolved gas in the free stream. This pressure is given by Henry's law namely

$$P_{G-S} = \alpha\beta \tag{11}$$

where α is the dissolved air content and β is the Henry's law constant. The dissolved air content was measured by a Van Slyke apparatus. Since we must have $P_c = P_{G-S}$ to assure no diffusion, this implies that the reference pressure (P_∞) from Equation (8) is given by

$$P_\infty = 1/2 \ \rho \ V_\infty^{\ 2} \ \sigma + P_{G-S} \tag{12}$$

It is apparent that diffusion cannot be entirely eliminated by this procedure since the cavity pressure is not precisely constant throughout the cavity. Since air was continuously forced into the water during a test the air content varied and so it was necessary to adjust the value of P_∞ in order to satisfy Equation (12). Furthermore, frequent shut-downs of the tunnel were required in order to reduce the air content.

Measurements of the volume flowrate of gas required to sustain ventilated cavities were made for velocities from 17 to 40 ft/sec and dimensionless cavity lengths from 1.0 to 3.0 for the two venturis. Nitrogen was used as the ventilation gas and the flowrate was measured by a Gilmont float-type flowmeter.

Results of the tests are shown in Figures 7 and 8 where the volume flowrate expressed as a dimensionless flow coefficient (C_Q) is shown as a function of dimensionless cavity length for several velocities. The data for C_Q were correlated by Equation (5) and the empirically determined constants are shown in Tables II and III for the first and second correlations together with the data for the ogives from Reference [11]. These correlations will be discussed in subsequent sections.

D. Determination of Cavity Geometry

The geometric characteristics of developed natural cavities were determined for both the full scale and 0.7 scale venturis. Cavity profiles were established for various operating conditions, and the surface area of the cavity (A_w) was determined by a technique similar to that employed in Reference [21]. The position of the cavity wall relative to the test section wall was determined by inserting a thin probe through the cavity until it pierced the cavity interface. This was done at two positions along the cavity. These two points together with the locations of the leading and trailing edges of the cavity were used to fit an arc to the contour of the cavity wall. The surface area was then determined by integration.

The cavity surface area was nondimensionalized by the square of the venturi diameter to form the area coefficient (C_A). The results are shown as a function of dimensionless cavity length (L/D) in Figure 9 for various velocities for the two venturis. It is seen that C_A is solely a function of L/D which is also characteristic of the ogives [17]. The data for C_A were approximated by Equation (4) and the empirically determined constants are shown in Table IV together with the ogive data from Reference [11]. It is seen that the exponent for L/D varies over the narrow range 1.09 - 1.19 for the three configurations.

In addition to the area coefficient, the ratio of minimum cavity diameter to venturi diameter (D_m/D) was determined as a function of L/D for the natural cavities on the full scale venturi. These results are shown in Figure 10.

IV. Application of the Entrainment Theory

The initial correlation made by the entrainment theory which is referred to as the first correlation did not include Weber number. These results are shown in Table II in which the data for the ogives were obtained from Reference [11] and [12]. The comparisons between the actual ogive data and values calculated from the correlations are given in References [11] and [12] for ΔT and References [20] and [22] for C_Q. The results for the second correlation, namely the correlation which did not include Froude number, are given in Table III. The comparisons between the experimental values of ΔT for the venturis and those calculated from the correlations are given in Table V. (The second correlation for the ogives was obtained after References [11] and [12] were published and is presented in this report for the first time.) A sketch of the ogives is shown in Figure 11 together with a description of the test conditions employed in the ogive tests.

Referring to the ogive data for C_Q, Nu, and ΔT for the first correlation (Table II), it is seen that the correlations are consistent i.e. the exponents of like terms have the same sign in corresponding correlations for the two ogives. Furthermore, the correlations for the ogive ΔT data are nearly independent of Froude number. This is perhaps not surprising since the Froude number was rather high in these tests. This result suggested the possibility that Froude number could be eliminated in the expressions for C_Q, Nu and ΔT and other parameters considered. Since the entrainment mechanism may depend upon surface tension effects it seemed reasonable to consider Weber number as a scaling parameter. Thus Froude number was replaced by Weber number and a second set of correlations for C_Q, Nu and ΔT were obtained as shown in Table III.

Referring to the ogive data for C_Q, Nu and ΔT in Table III, it is seen that the exponents of like terms have the same sign and thus corresponding correlations for the two ogives are consistent. Furthermore, the exponents on the Weber number terms in Table III are consistently higher than the corresponding exponents on the Froude number terms in Table II. Perhaps this indicates that in this instance the Weber number is better than Froude number as a scaling parameter.

As indicated in the foregoing discussion, the data for the two ogive families are consistent within the context of the entrainment theory for both correlations i.e. exponents of like terms in the equations have the same sign. However, referring to Tables II and III it is seen that the venturi correlations do not exhibit the same trends as the corresponding ogive correlations in all cases. For example, in the first correlation (Table II) the Froude number exponent for the venturis is negative in the expressions for C_Q and Nu whereas the same set of exponents for the ogives is positive. Similarly, in the second correlation (Table III) the Weber number exponent displays the same inconsistencies. Furthermore, the sign of the Reynolds number exponent in the second correlation for C_Q is positive for the venturis whereas the same exponent for the ogives is negative. Comparing the venturi correlation for ΔT with those for the ogives we see that the sign of the exponents for the cavity length, Reynolds and Prandtl number terms are the same but the signs of the Froude and Weber number exponents are opposite to the signs of the corresponding exponents for the ogives.

It is interesting to compare the exponents on the Prandtl number for the various correlations given in Tables II and III. Referring to the venturi correlations it is seen that Prandtl number exponent for the ΔT equation is -0.04 and -0.46 for the first and second correlations, respectively. Thus the exponent has increased by an order of magnitude from the first to the second correlation. In contrast to this result, the Prandtl number exponent for the ogive ΔT correlation changes from -0.85 to -0.64 for the zero caliber ogive and from -0.41 to -0.31 for the quarter caliber ogive in going from the first to the second correlation. The much larger change in the Prandtl number exponent for the venturi is due to the introduction of surface tension into the ΔT correlation which has a large variation for the fluids used in the correlation namely Freon 114, nitrogen, and hydrogen. The magnitude of the Prandtl number exponent for the second correlation, namely 0.46 is more typical of heat transfer data. Perhaps this suggests that the second correlation is better than the first correlation for the venturis.

The various entrainment theory correlations for ΔT are compared in Table VI for the case of constant fluid properties where ΔT has the form

$$\Delta T_{max} = C\left(\frac{L}{D}\right)^{M1} V_{\infty}^{M2} D^{M3} \tag{13}$$

in which the constant C is different for each configuration. In addition, two of the B factor correlations are shown in Table VI. (Apparently, these are the only B factor correlations available for the venturis and ogives which include size, i.e. D, directly as a parameter. Weir [12] has summarized the various B factor correlations.) Comparing the first and second entrainment method correlations for a given configuration with each other indicates that the two correlations give nearly the same exponents for like terms. Both of the correlations for the venturis show that the size effect is very small. The B factor correlations for the venturis shows a larger effect with ΔT varying as the 0.2 power of D. The exponent on L/D varies between 0.26 and 0.36 for the venturis and quarter caliber ogives whereas the zero caliber ogives display a much larger effect for the average L/D exponent is 0.85. All of the configurations and correlations indicate that ΔT increases with velocity with the exception of the zero caliber ogive. In addition, all of the configurations and correlations indicate that ΔT increases with or is not affected by size with the exception of the zero caliber ogive which shows a decrease of ΔT with size. Thus the zero caliber ogive tends to be the exception when examined for the case of constant fluid properties. However, as indicated by previous arguments the zero and quarter caliber ogives are consistent within the context of entrainment theory i.e. the signs of the exponents of like terms are the same in the equations for C_Q, Nu and ΔT expressed in dimensionless form.

V. Conclusions

The major conclusions from this investigation and pertinent conclusion from the ogive investigation of Reference [11] are:

(1) The entrainment theory appears to be a reasonable alternative to the B factor method.

(2) The temperature depression for the quarter caliber ogives increases with T_∞, L/D, V_∞, and D. This result is in general agreement with other investigations of quarter caliber ogives, hydrofoils, and venturis.

(3) The temperature depression for the zero caliber ogives increases with T_∞ and L/D but tends to decrease with V_∞ and D.

(4) Both the first and second correlations show consistent results for the ogives within the context of the entrainment theory in that the exponents of like terms have the same sign in the expressions for C_Q, Nu and ΔT.

(5) The ΔT expressions for the ogives from the first correlation show that the Froude number term is very small and can be neglected. This result was the basis for obtaining the second correlation in which the Froude number was replaced by Weber number.

(6) In general, within the context of the entrainment theory the venturi expressions for ΔT, C_Q and Nu for both the first and second correlations do not show the same trends as those for the ogives.

(7) The cavitation number is independent of L/D for the venturis whereas it is a single valued function of L/D in the case of the ogives.

(8) For the venturis, the magnitude of the Prandtl number exponent for the second correlation appears to be more consistent with other heat transfer data than does the Prandtl number exponent for the first correlation. Perhaps this suggests that the second correlation is better than the first for the venturi data.

VI. Acknowledgments

The major portion of the technical work on the research program was sponsored by the National Aeronautics and Space Administration under Grant NGL 39-009-001. Mr. Werner R. Britsch of NASA is the technical monitor of this grant. All reports as a result of this grant do not require security clearance from NASA.

VII. References

[1] Stahl, H. A. and Stepanoff, A. J., "Thermodynamic Aspects of Cavitation in Centrifugal Pumps," Trans. ASME, Vol. 78, 1956.

[2] Fisher, R. C., Discussion of "A Survey of Modern Centrifugal Pump Practice for Oilfield and Oil Refining Services," by N. Tetlou, Proc. Inst. Mech. Engrs., Vol. 152, 1945.

[3] Jacobs, R. B., "Prediction of Symptoms of Cavitation," J. Res. NBS, Vol. 65C, No. 3, 1961.

[4] Acosta, A. J. and Hollander, A., "Remarks on Cavitation in Turbomachines," Hydromechanics Laboratory, California Institute of Technology, Report 79.3, October 1959.

[5] Gelder, T. F., Ruggeri, R. S., and Moore, R. D., "Cavitation Similarity Considerations Based on Measured Pressure and Temperature Depressions in Cavitated Regions of Freon 114," NASA TN D-3509, 1966.

[6] Moore, R. D. and Ruggeri, R. S., "Prediction of Thermodynamic Effects of Developed Cavitation Based on Liquid-Nitrogen and Freon 114 Data in Scaled Venturis," NASA TN D-4899, 1962.

[7] Hord, J., Anderson, L. M., and Hall, W. J., "Cavitation in Liquid Cryogens, Volume I -- Venturi," NASA CR-2054, 1972.

[8] Hord. J., "Cavitation in Liquid Cryogens, Volume II -- Hydrofoil," NASA CR-2156, January 1973.

[9] Hord, J., "Cavitation in Liquid Cryogens, Volume III -- Ogives," NASA CR-2242, May 1973.

[10] Hord, J., "Cavitation in Liquid Cryogens, Volume IV -- Combined Correlations for Venturi, Hydrofoil, Ogives, and Pumps," NASA CR-2448, 1974.

[11] Holl, J. W., Billet, M. L., and Weir, D. S., "Thermodynamic Effects on Developed Cavitation," Proceedings of the Symposium on Cavity Flows, ASME Fluids Engr. Conf., Minneapolis, Minn., May 1975, pp. 101-110.

[12] Weir, D. S., "An Experimental and Theoretical Investigation of Thermodynamic Effects on Developed Cavitation," M.S. Thesis, The Pennsylvania State University, May 1975, (also ARL Technical Memorandum 75-34).

[13] Becket, R. and Hunt, J., Numerical Calculations and Algarithms, McGraw-Hill Book Company, New York, 1967.

[14] Weir, D. S., Billet, M. L. and Holl, J. W., "The 1.5 inch Ultra-High-Speed Cavitation Tunnel at the Applied Research Laboratory of the Pennsylvania State University," ARL Technical Memorandum 75-188, July 10, 1975.

[15] Gelder, T. F., Moore, R. D., and Ruggeri, R. S., "Incipient Cavitation of Freon 114 in a Tunnel Venturi," NASA TN D-2662, February 1965.

[16] Edmonds, D. K., Hord, J., and Millhiser, D. R., "Cavitation Inception in Liquid Nitrogen and Liquid Hydrogen Flowing in a Venturi," NASA CR-72285, August 1967.

[17] Billet, M. L., Holl, J. W. and Weir, D. S., "Geometric Description of Developed Cavities on Zero and Caliber Ogive Bodies," ARL Technical Memorandum 74-136, May 6, 1974.

[18] Reichardt, H., "The Laws of Cavitation Bubbles at Axially Symmetrical Bodies in a Flow," Reports and Translations No. 766, Office of Naval Research, October 1947.

[19] Weir, D. S., "The Effect of Velocity, Temperature, and Blockage on the Cavitation Number for a Developed Cavity," Proceedings of the 1975 Cavitation and Polyphase Flow Forum, ASME Fluids Engineering Conf., Minneapolis, Minn., May 1975, pp. 7-10.

[20] Billet, M. L., and Weir, D. S., "The Effect of Gas Diffusion on the Flow Coefficient for a Ventilated Cavity," Proceedings of the Symposium on Cavity Flows, ASME Fluids Engr. Conf., Minneapolis, Minn., May 1975, pp. 95-100.

[21] Billet, M. L., "Thermodynamic Effects on Developed Cavitation in Water and Freon 113," M.S. Thesis, The Pennsylvania State University, March 1970.

[22] Billet, M. L. and Weir, D. S., "The Effect of Gas Diffusion and Vaporization on the Entrainment Coefficient for a Ventilated Cavity," ARL Technical Memorandum 74-15, January 24, 1974.

[23] Ruggeri, R. S. and Gelder, T. F., "Cavitation and Effective Liquid Tension of Nitrogen in a Tunnel Venturi," NASA TN D-2088, February 1964.

December 11, 1975
MLB:JWH:DSW:jep

Table I Tabulation of Experimental Data for the Venturis
(Fluid: Water Temperature: 70 °F)

Part A Tabulation of σ Data for Developed Cavitation

MODEL DIAMETER IN.	CAVITY LENGTH IN.	VELOCITY FT/SEC	CAVITATION NUMBER (σ)
0.975	1.00	19.1	2.26
0.975	1.00	16.4	2.16
0.975	2.00	17.3	2.11
0.975	2.00	16.4	2.08
0.975	3.00	16.8	2.03
0.975	3.00	18.5	1.93
0.975	1.00	26.0	2.50
0.975	1.00	27.4	2.41
0.975	2.00	27.6	2.41
0.975	3.00	25.1	2.38
0.975	3.00	27.0	2.51
1.378	1.00	19.1	2.30
1.378	1.00	18.9	2.35
1.378	1.50	18.4	2.34
1.378	1.50	18.1	2.33
1.378	1.00	29.0	2.56
1.378	1.00	27.9	2.58
1.378	1.50	28.5	2.27
1.378	1.50	29.4	2.28
1.378	2.00	17.7	2.38
1.378	2.00	17.7	2.27
1.378	1.00	40.0	2.41
1.378	1.00	39.3	2.54

Table I Tabulation of Experimental Data for the Venturis
(Fluid: Water Temperature: 70 °F)

Part B Tabulation of σ Data for Limited Cavitation

MODEL DIAMETER IN.	REYNOLDS NUMBER	VELOCITY FT/SEC	CAVITATION NUMBER (σ)
1.378	2.5×10^5	23.1	3.50
1.378	3.5×10^5	32.3	3.05
1.378	3.5×10^5	32.3	3.40
1.378	4.5×10^5	41.5	3.10
1.378	4.5×10^5	41.5	3.55
1.378	5.9×10^5	54.5	3.20
1.378	5.9×10^5	54.5	3.25

Table I Tabulation of Experimental Data for the Venturis
(Fluid: Water Temperature: 70 °F)

Part C Tabulation of C_Q Data

MODEL DIAMETER IN.	CAVITY LENGTH IN.	VELOCITY FT/SEC	C_Q (Measured)	C_{Q_2}	C_{Q_1}
1.378	1.378	19.2	.0151	.0166	.0167
1.378	1.378	18.9	.0147	.0166	.0167
1.378	2.067	18.4	.0262	.0257	.0256
1.378	2.067	18.1	.0268	.0256	.0254
1.378	2.756	17.7	.0374	.0349	.0344
1.378	2.756	17.7	.0353	.0349	.0344
1.378	1.378	29.0	.0190	.0186	.0187
1.378	1.378	27.9	.0198	.0184	.0185
1.378	2.067	28.5	.0312	.0289	.0288
1.378	2.067	29.4	.0297	.0291	.0290
1.378	1.378	40.0	.0185	.0202	.0204
1.378	1.378	39.3	.0201	.0202	.0203
0.975	0.975	19.1	.0139	.0136	.0136
0.975	0.975	16.4	.0138	.0131	.0130
0.975	1.950	17.3	.0280	.0284	.0278
0.975	1.950	16.4	.0288	.0280	.0274
0.975	2.925	16.8	.0376	.0439	.0425
0.975	0.975	26.1	.0154	.0148	.0148
0.975	0.975	27.5	.0149	.0150	.0150
0.975	1.950	27.6	.0323	.0321	.0315
0.975	2.925	25.2	.0493	.0489	.0475
0.975	2.925	27.0	.0488	.0498	.0484

C_{Q_1} = C_Q calculated by first correlation.

C_{Q_2} = C_Q calculated by second correlation.

Table I Tabulation of Experimental Data for the Venturis
(Fluid: Water Temperature: 70 °F)

Part D Tabulation of C_A Data

MODEL DIAMETER IN.	CAVITY LENGTH IN.	VELOCITY FT/SEC	C_A
1.378	1.378	50.0	2.55
1.378	1.378	30.0	2.60
1.378	2.067	50.0	3.99
1.378	2.067	30.0	4.10
1.378	2.756	50.0	5.68
1.378	2.756	30.0	5.60
1.378	4.134	50.0	7.23
1.378	4.134	30.0	7.11
0.975	1.950	30.0	5.56

Table I **Tabulation of Experimental Data for the Venturis**
(Fluid: Water Temperature: 70 °F

Part E **Tabulation of Minimum Dimensionless Cavity Diameter Data**

MODEL DIAMETER IN.	CAVITY LENGTH IN.	VELOCITY FT/SEC	D_m/D	L/D
1.378	1.378	28.7	.925	1.0
1.378	1.378	18.3	.930	1.0
1.378	2.067	28.7	.894	1.5
1.378	2.067	18.3	.915	1.5
1.378	2.756	28.7	.930	2.0
1.378	2.756	18.3	.900	2.0
1.378	3.445	28.7	.885	2.5
1.378	3.445	18.3	.929	2.5

Table II

Constants and Exponents for Entrainment Theory-First Correlation

Model	Quantity	Eq. No.	Constant C_2, C_3 or C_4	L/D Exp.	Re Exp.	Fr Exp.	We Exp.	Pr Exp.	Pe Exp.
Venturi	C_Q	5	0.676×10^{-4}	1.06	0.48	-0.21	0	----	----
	Nu	6	0.611×10^{-3}	-0.39	1.36	-0.59	0	0.04	----
	ΔT_{max}	7	0.421×10^{-1}	0.36	-0.88	0.38	0	-0.04	1.0
Zero-Caliber* Ogive	C_Q	5	0.424×10^{-2}	0.69	0.16	0.13	0	----	----
	Nu	6	0.148×10^{-3}	-1.33	1.39	0.15	0	0.85	----
	ΔT_{max}	7	6.221	0.83	-1.23	-0.02	0	-0.85	1.0
Quarter-Caliber* Ogive	C_Q	5	0.320×10^{-4}	0.74	0.46	0.26	0	----	----
	Nu	6	0.464×10^{-2}	-0.70	1.03	0.30	0	0.41	----
	ΔT_{max}	7	0.335×10^{-2}	0.26	-0.57	-0.04	0	-0.41	1.0

* These correlations are the same as those given in Reference [11] except for small adjustments in the constants due to the use of new fluid property data.

Table III

Constants and Exponents for Entrainment Theory-Second Correlation

Model	Quantity	Eq. No.	Constant C_2, C_3 or C_4	L/D Exp.	Re Exp.	Fr Exp.	We Exp.	Pr Exp.	Pe Exp.
Venturi	C_Q	5	0.618×10^{-5}	1.09	0.88	0	-0.62	----	----
	Nu	6	0.275×10^{-5}	-0.32	2.33	0	-1.67	0.46	----
	ΔT_{max}	7	0.854	0.32	-1.45	0	1.05	-0.46	1.0
Zero-Caliber Ogive	C_Q	5	0.225×10^{-1}	0.69	-0.10	0	0.40	----	----
	Nu	6	0.415×10^{-2}	-1.37	0.90	0	0.68	0.64	----
	ΔT_{max}	7	1.183	0.87	-1.00	0	-0.28	-0.64	1.0
Quarter-Caliber Ogive	C_Q	5	0.836×10^{-3}	0.74	-0.06	0	0.79	----	----
	Nu	6	0.271	-0.70	0.41	0	0.93	0.31	----
	ΔT_{max}	7	1.498×10^{-3}	0.26	-0.47	0	-0.14	-0.31	1.0

Table IV

Constants and Exponents for C_A Correlations

Model	Constant C_1	L/D Exponent
Venturi	2.63	1.09
Zero-Caliber Ogive*	4.59	1.19
Quarter-Caliber Ogive*	2.06	1.18

$$C_A = C_1(L/D)^a$$

* Data from Reference [11].

Table V

Comparison of Measured ΔT with Calculated ΔT for the Venturis

FLUID	MODEL DIAMETER IN.	CAVITY LENGTH IN.	VELOCITY FT/SEC	FLUID TEMP. (°R)	TEMPERATURE DEPRESSION MEASURED ΔT (°F)	PREDICTED ΔT_2 (°F)	ΔT_1 (°F)
HYDROGEN	.975	2.00	102.1	35.8	3.19	2.54	2.75
	.975	2.50	98.8	35.7	2.61	2.67	2.93
	.975	3.25	99.8	35.7	3.38	2.92	3.24
	.975	3.25	143.3	37.2	4.27	4.29	4.54
	.975	1.75	150.9	36.7	3.59	3.44	3.54
	.975	2.75	149.6	36.6	4.94	3.91	4.11
	.975	2.50	163.1	40.3	4.88	5.95	6.00
	.975	3.25	166.8	40.2	5.42	6.50	6.61
	.975	3.50	168.4	40.3	5.47	6.78	6.90
	.975	1.75	172.6	37.1	4.64	3.90	3.95
	.975	2.63	174.9	37.0	5.43	4.45	4.57
	.975	3.25	173.0	36.1	6.05	4.65	4.83
	.975	3.25	173.0	37.0	5.75	4.72	4.90
	.975	1.25	187.6	40.4	4.05	5.24	5.06
	.975	2.00	190.3	37.2	5.24	4.34	4.3
	.975	2.00	192.7	37.2	5.32	4.39	4.41
	.975	3.25	190.7	37.2	6.18	5.12	5.25
	.975	3.50	194.0	37.1	5.69	5.24	5.39
	.975	2.00	192.1	40.7	5.05	6.37	6.23
	.975	3.25	189.8	40.4	6.18	7.21	7.21
	.975	3.25	192.4	40.5	6.35	7.35	7.34
FREON 114	.975	1.60	31.1	60.7	6.80	6.91	7.26
	.975	1.60	32.5	79.9	8.90	9.30	9.64
	.975	1.60	22.0	39.1	4.00	4.09	4.48
	.975	1.60	22.7	60.0	5.40	5.65	6.14
	.975	1.60	22.9	79.7	7.80	7.50	8.07
	.975	1.60	44.3	60.3	8.80	8.51	8.62
	.975	1.60	44.5	80.1	10.50	11.28	11.31
	.975	0.70	54.2	60.7	5.20	5.58	5.62
	.975	3.00	26.9	60.7	7.20	7.77	8.51
HYDROGEN	.975	1.25	151.4	36.9	2.58	3.13	3.18
	.975	2.00	151.9	37.0	3.54	3.75	3.87
	.975	3.25	152.8	37.1	4.17	4.41	4.64
	.975	1.25	128.7	38.6	3.43	3.44	3.51
	.975	2.00	127.1	38.7	3.71	4.02	4.18
	.975	3.25	130.5	38.8	4.19	4.85	5.12
	.975	1.25	139.7	40.5	4.28	4.44	4.41
	.975	2.00	144.1	40.6	5.05	5.29	5.34
	.975	3.25	144.8	41.0	5.74	6.49	6.65

Table V Comparison of Measured ΔT with Calculated ΔT for the Venturis (Cont.)

FLUID	MODEL DIAMETER IN.	CAVITY LENGTH IN.	VELOCITY FT/SEC	FLUID TEMP. (°R)	TEMPERATURE DEPRESSION MEASURED ΔT (°F)	PREDICTED ΔT_2 (°F)	PREDICTED ΔT_1 (°F)
HYDROGEN	.975	1.25	196.8	37.5	3.53	3.94	3.87
	.975	2.00	199.4	37.6	4.50	4.70	4.69
	.975	3.25	204.0	37.5	6.24	5.51	5.60
	.975	1.25	195.6	38.6	4.47	4.42	4.31
	.975	2.00	197.4	38.6	5.50	5.20	5.16
	.975	3.25	195.8	38.4	6.44	5.93	6.02
	.975	1.25	190.4	40.7	5.24	5.46	5.24
	.975	2.00	189.4	40.7	5.69	6.29	6.17
	.975	3.25	189.7	40.6	6.70	7.37	7.37
	.975	1.25	196.2	37.6	4.98	3.98	3.91
	.975	1.25	202.9	40.8	6.25	5.72	5.45
	.975	2.00	202.8	40.7	6.52	6.56	6.38
	.975	3.25	204.7	40.9	7.69	7.95	7.86
	.975	1.25	197.6	38.5	5.11	4.41	4.30
	.975	2.00	198.4	38.5	5.38	5.16	5.12
	.975	3.25	201.1	38.9	6.26	6.36	6.41
	.975	1.25	139.2	38.8	3.97	3.68	3.72
	.975	2.00	141.2	38.7	4.77	4.31	4.43
	.975	3.25	143.8	39.7	5.36	5.66	5.87
	.975	1.25	155.4	37.1	3.53	3.25	3.28
	.975	2.00	155.0	36.7	4.35	3.66	3.77
	.975	3.25	153.9	37.2	5.45	4.70	4.96
	.975	2.00	151.6	40.8	4.45	5.60	5.61
	.975	3.25	153.2	40.9	5.24	6.67	6.80
	.975	1.25	111.0	36.5	2.79	2.48	2.60
	.975	2.00	113.1	36.5	2.95	2.92	3.12
NITROGEN	.975	3.25	35.2	140.1	3.00	2.61	2.52
	.975	3.25	50.5	139.8	3.10	3.18	2.96
	.975	3.25	45.8	150.7	4.30	5.15	4.73
	.975	3.25	65.4	160.4	8.70	10.11	8.68
	.975	3.25	74.1	160.7	8.60	11.06	9.35
	.975	3.25	73.1	150.5	6.50	6.77	5.92
	.975	3.25	73.1	140.9	4.20	4.23	3.78
	.975	3.25	72.8	140.7	4.30	4.18	3.73
	.975	3.25	49.7	140.5	3.30	3.28	3.05
	.975	3.25	48.2	140.5	3.60	3.22	3.01
FREON 114	1.378	2.75	31.4	27.5	5.40	4.67	4.68
	1.378	2.75	31.8	59.1	7.30	7.49	7.50
	1.378	2.75	31.7	78.8	9.20	9.88	9.79
	1.378	2.75	18.9	7.7	2.70	2.49	2.62
	1.378	2.75	18.3	27.1	3.30	3.40	3.60
	1.378	2.75	18.9	60.7	5.00	5.59	5.91
	1.378	2.75	43.2	29.7	7.30	5.86	5.68
	1.378	2.75	43.9	62.5	9.10	9.56	9.23
	1.378	0.50	33.1	59.1	3.90	4.39	4.08
	1.378	1.25	32.8	59.1	6.30	5.89	5.69
	1.378	4.00	30.2	59.1	8.00	8.21	8.39

Table V Comparison of Measured ΔT with Calculated ΔT for the Venturis (Cont.)

FLUID	MODEL DIAMETER IN.	CAVITY LENGTH IN.	VELOCITY FT/SEC	FLUID TEMP. (°R)	TEMPERATURE DEPRESSION MEASURED ΔT (°F)	PREDICTED ΔT_2 (°F)	ΔT_1 (°F)
NITROGEN	1.378	1.00	20.4	140.0	1.10	1.16	1.06
	1.378	2.00	20.1	140.0	1.30	1.44	1.35
	1.378	4.00	19.2	140.0	1.80	1.76	1.71
	1.378	4.00	25.1	140.4	2.30	2.12	1.99
	1.378	4.00	31.5	141.0	2.70	2.51	2.30
	1.378	4.00	42.0	142.6	3.00	3.23	2.87

ΔT_1 = ΔT predicted by first correlation.

ΔT_2 = ΔT predicted by second correlation.

Table VI

ΔT Correlations for Constant Fluid Properties

BOUNDARY	SOURCE	FLUIDS	CORRELATION METHOD	EQUATIONS FOR ΔT
Venturi	This study, Moore and Ruggeri 1968 and Hord et al. 1972	Hydrogen Nitrogen Freon 114	Entrainment Method First Correlation	$\Delta T = C(L/D)^{0.36}\ V_\infty^{0.5}\ D^{-0.07}$
Venturi		Hydrogen Nitrogen Freon 114	Entrainment Method Second Correlation	$\Delta T = C(L/D)^{0.32}\ V_\infty^{0.6}\ D^{0.07}$
Venturi	Moore and Ruggeri 1968	Hydrogen Freon 114	B Factor Method	$\Delta T = C(L/D)^{0.3}\ V_\infty^{0.8}\ D^{0.2}$
Zero Caliber Ogive	This study, and Holl, Billet and Weir 1975.	Water Freon 113	Entrainment Method First Correlation	$\Delta T = C(L/D)^{0.83}\ V^{-0.25}\ D^{-0.22}$
Zero Caliber Ogive			Entrainment Method Second Correlation	$\Delta T = C(L/D)^{0.87}\ V^{-0.28}\ D^{-0.14}$
Quarter Caliber Ogive			Entrainment Method First Correlation	$\Delta T = C(L/D)^{0.26}\ V^{0.39}\ D^{0.45}$
Quarter Caliber Ogive			Entrainment Method Second Correlation	$\Delta T = C(L/D)^{0.26}\ V^{0.39}\ D^{0.46}$
Quarter Caliber Ogive	Hord 1973	Hydrogen Nitrogen	B Factor Method	$\Delta T = C(L/D)^{0.34}\ V^{0.21}\ D^{0.94}$

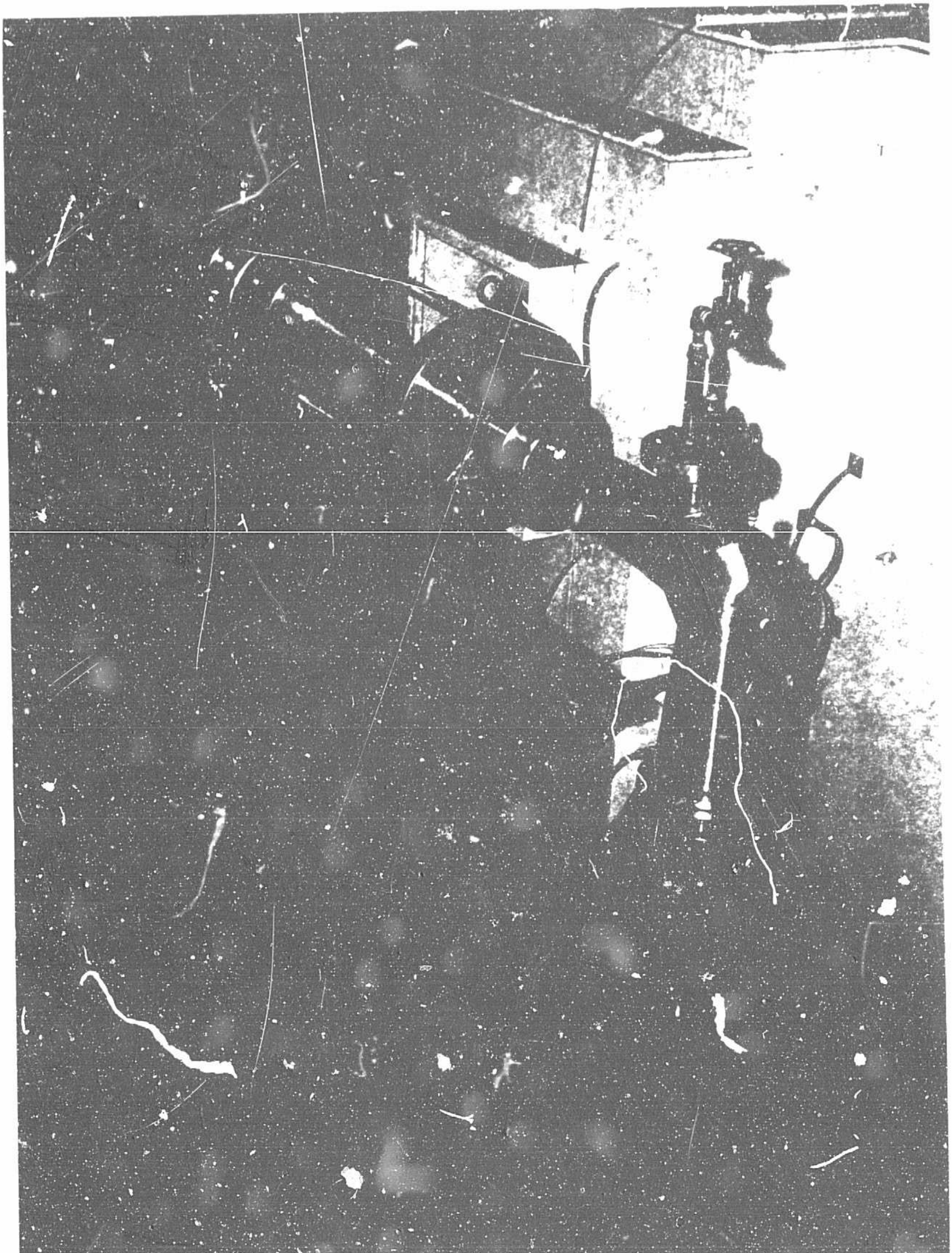

Figure 1 Photograph of the Ultra-High Speed Cavitation Tunnel

Figure [illegible] - Photograph of Venturis: A. 0.7 Scale Venturi (0.975-inch Diameter) and B. Full Scale Venturi (1.378-inch Diameter) with Air Injection Ring

December 11, 1975
MLB:JWH:DSW:jep

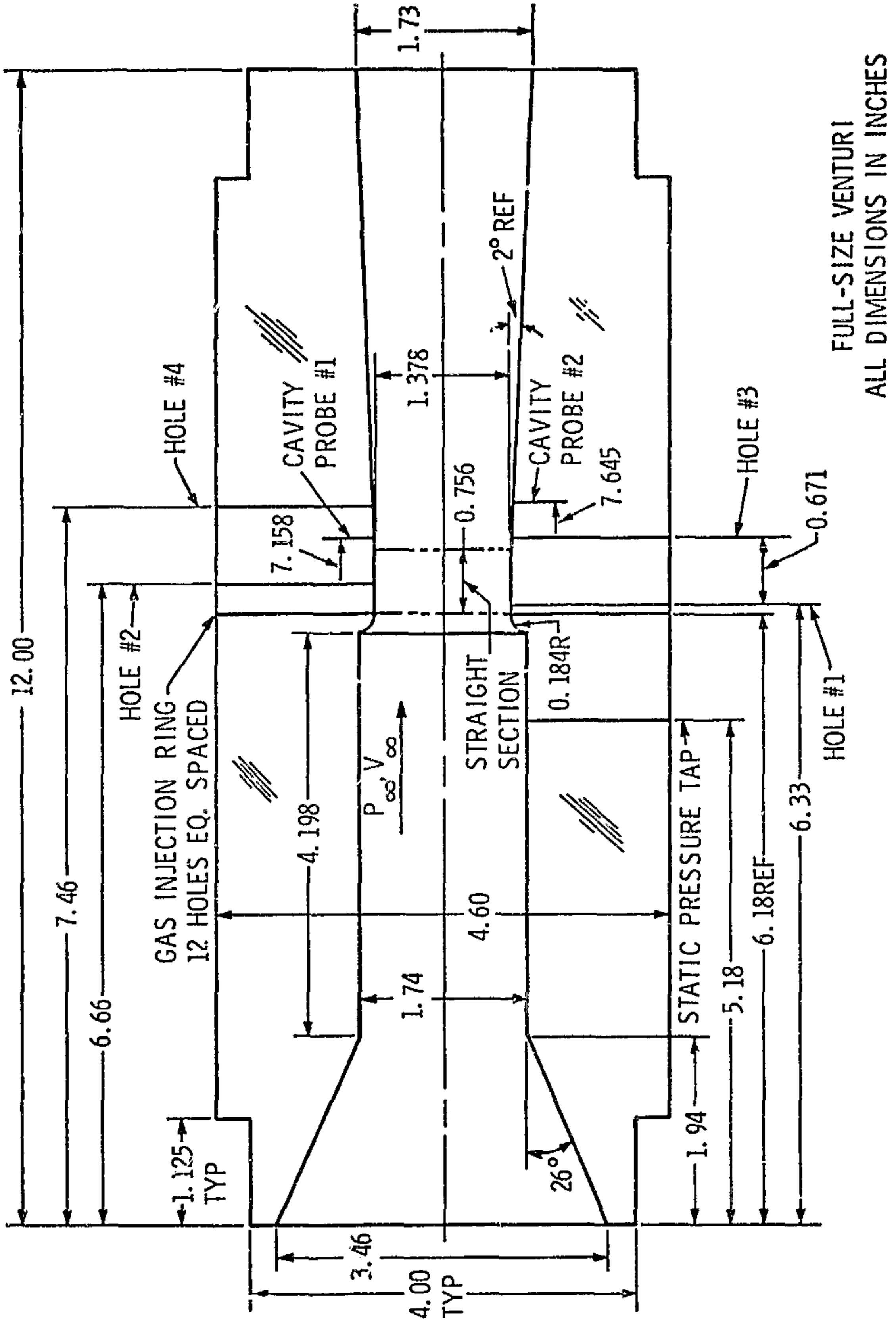

Figure 3 - Sketch of the Full Scale Venturi

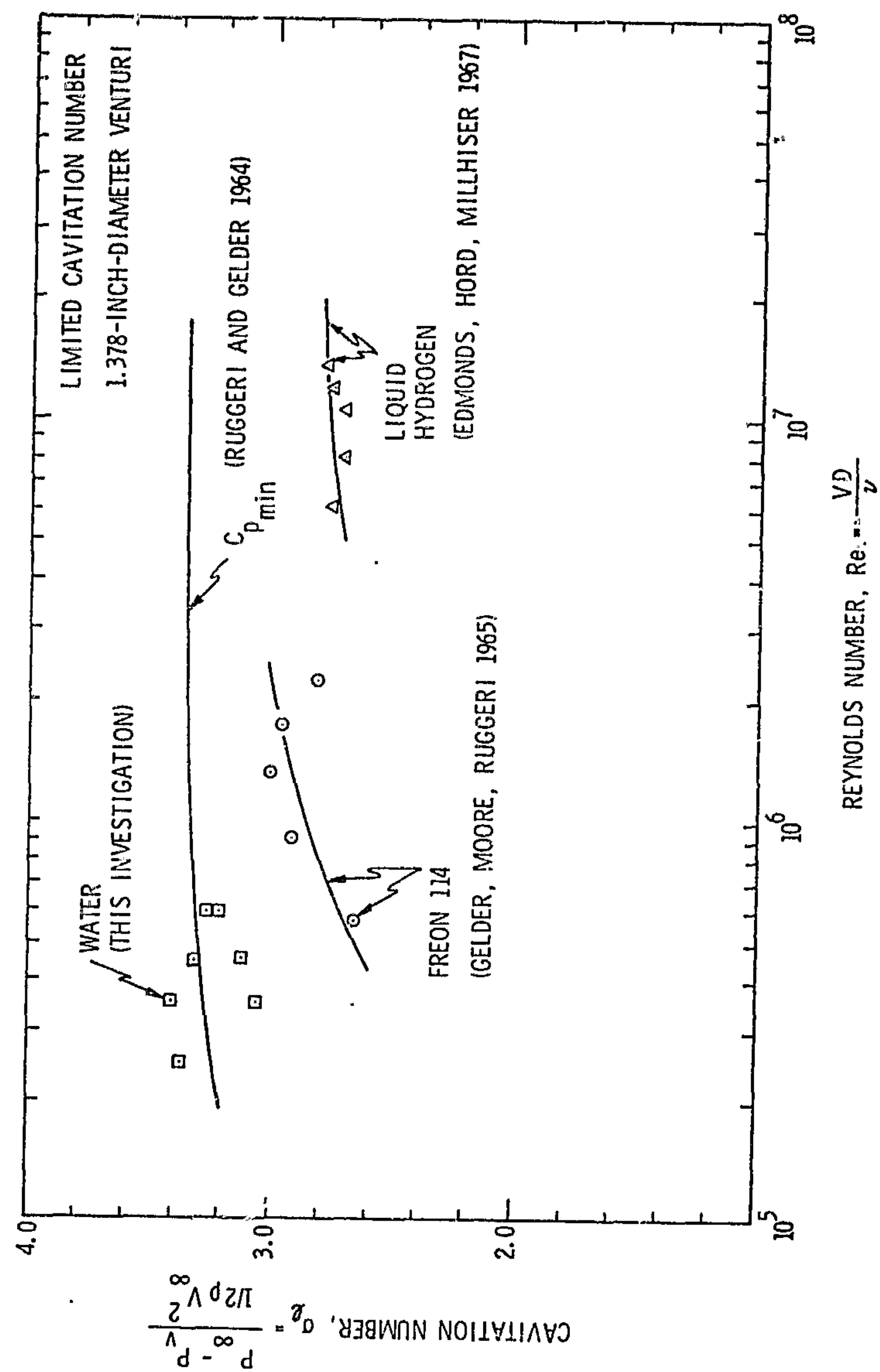

Figure 4 - Limited Cavitation Number Versus Reynolds Number for Venturis

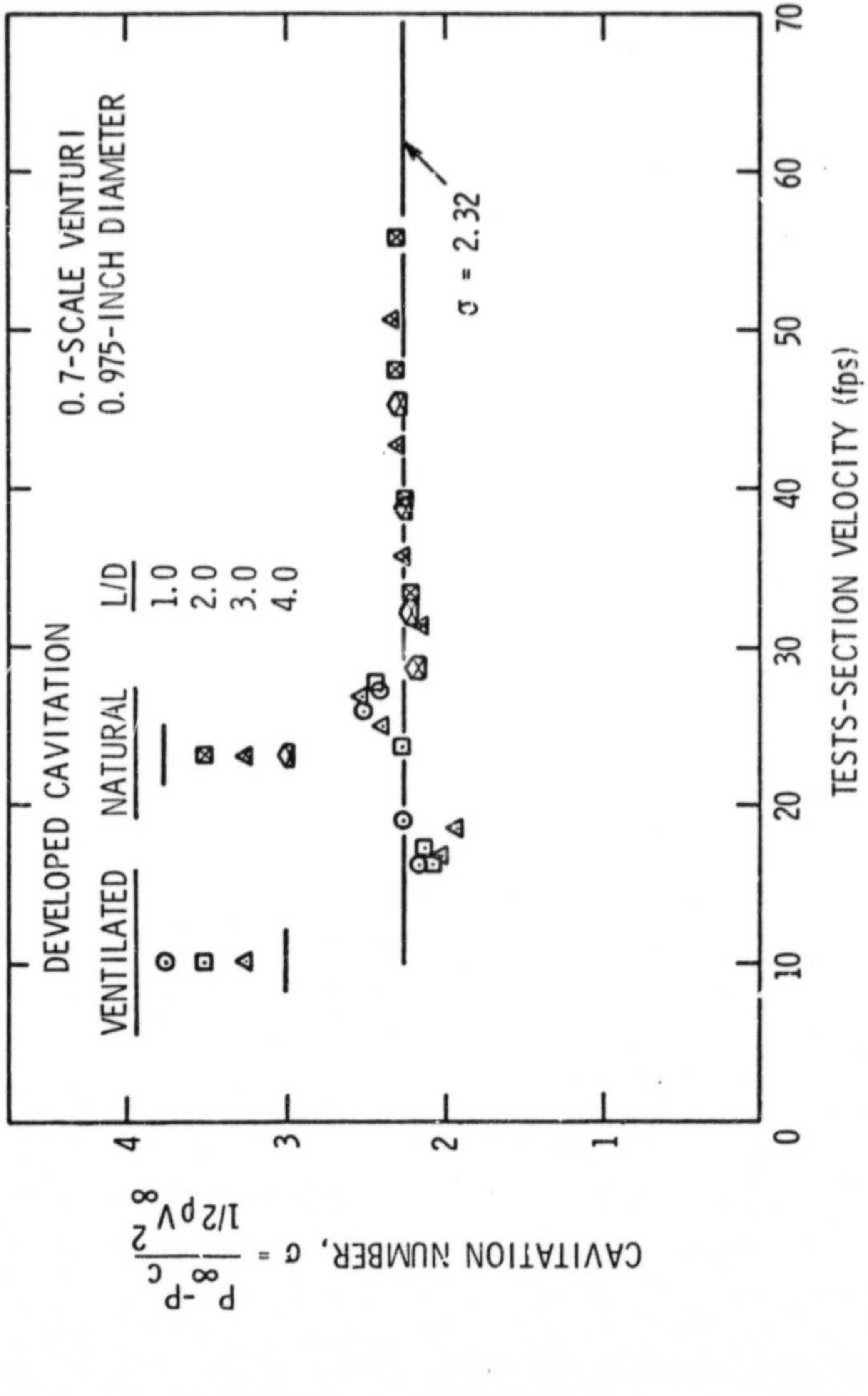

Figure 5 - Cavitation Number for Developed Cavitation on 0.7 Scale Venturi

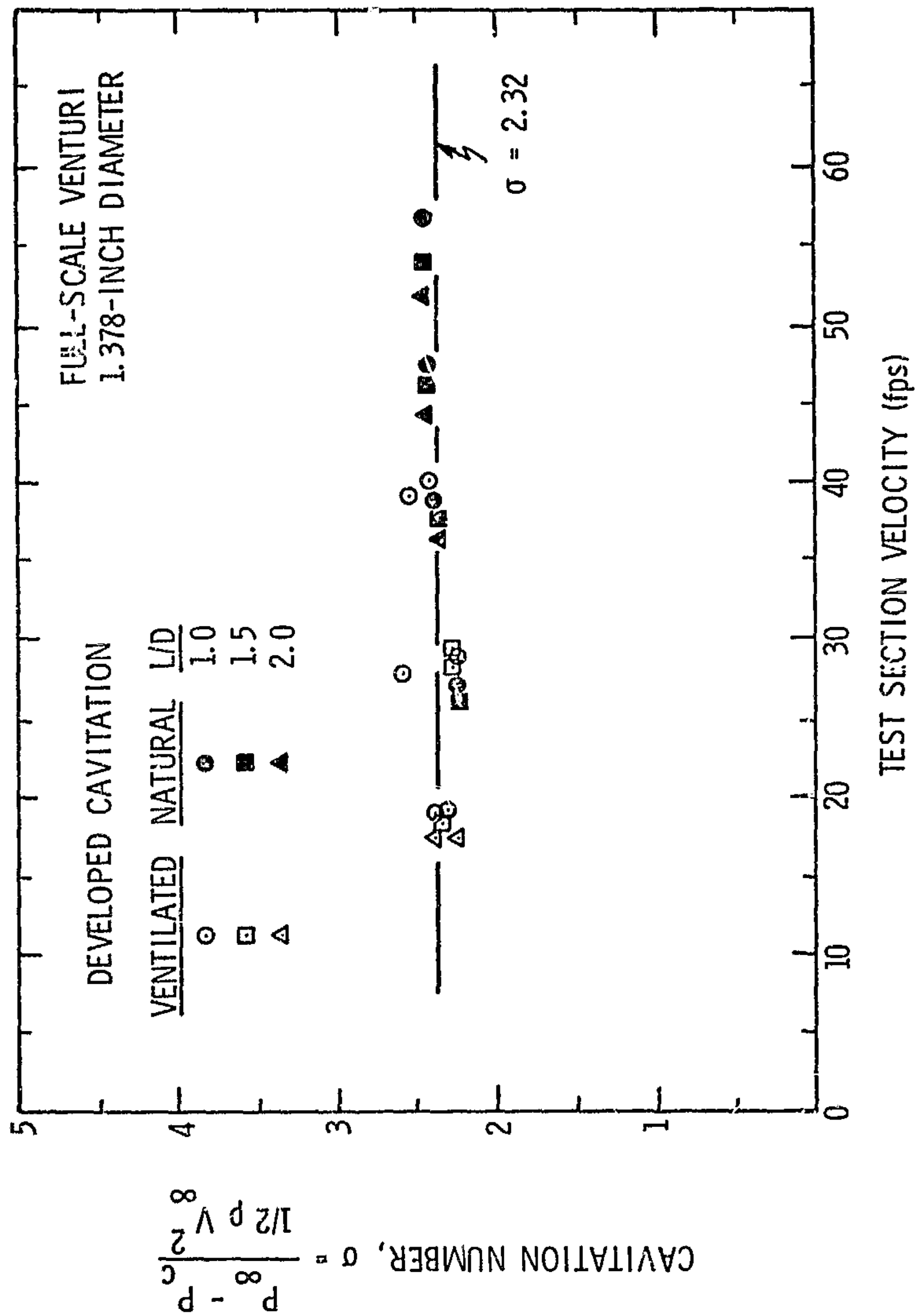

Figure 6 - Cavitation Number for Developed Cavitation on Full Scale Venturi

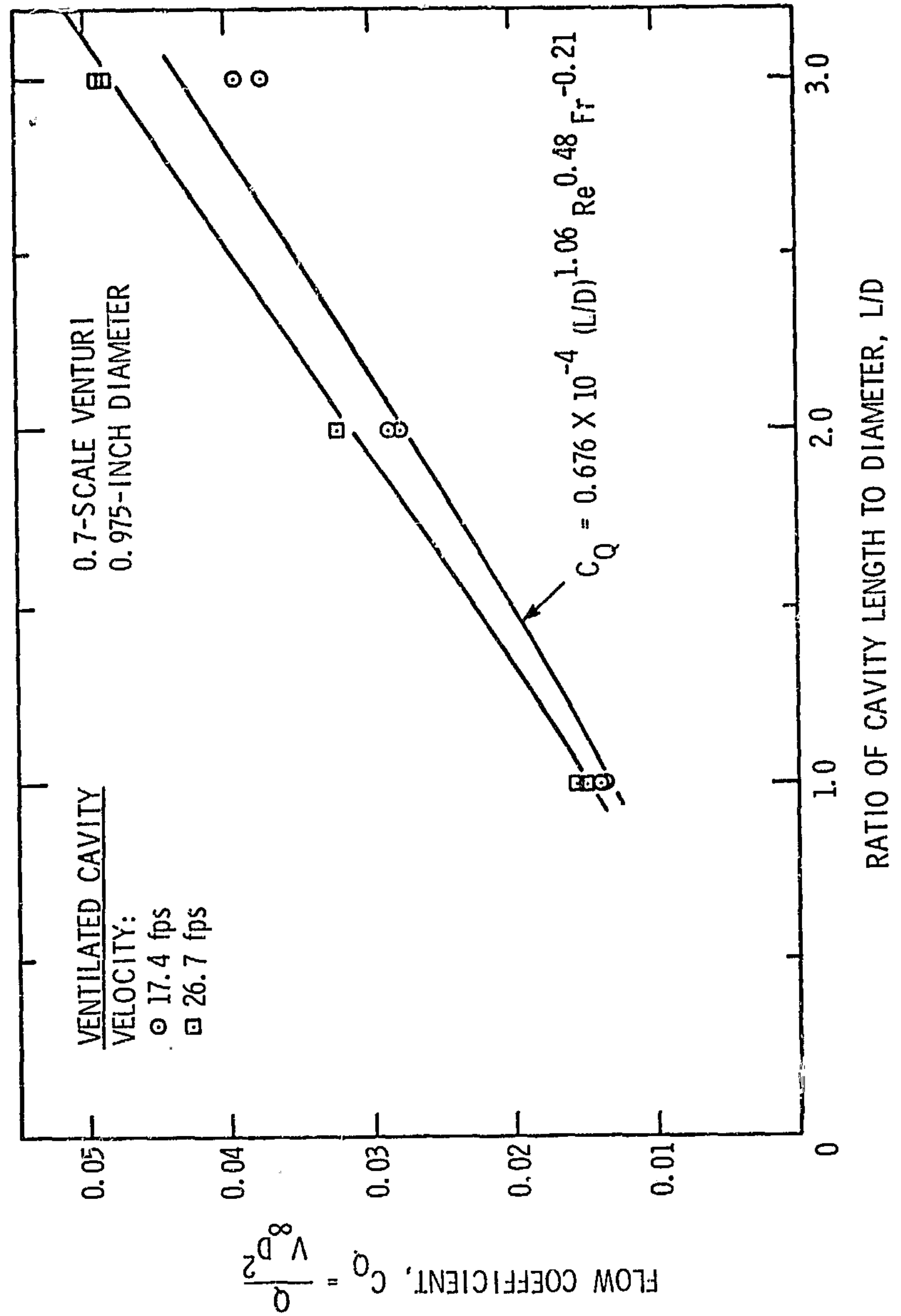

Figure 7 - Flow Coefficient for 0.7 Scale Venturi

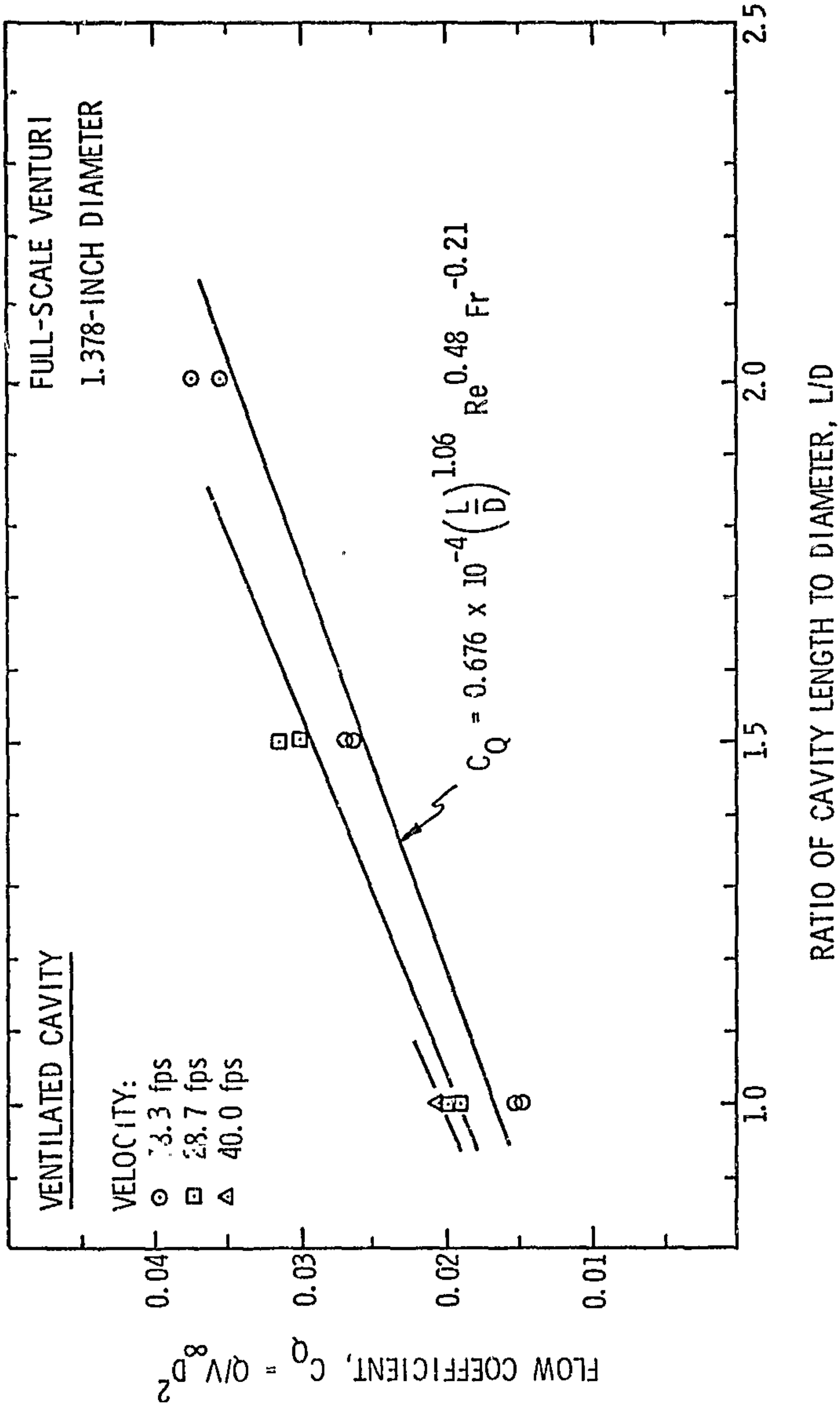

Figure 8 - Flow Coefficient for Full Scale Venturi

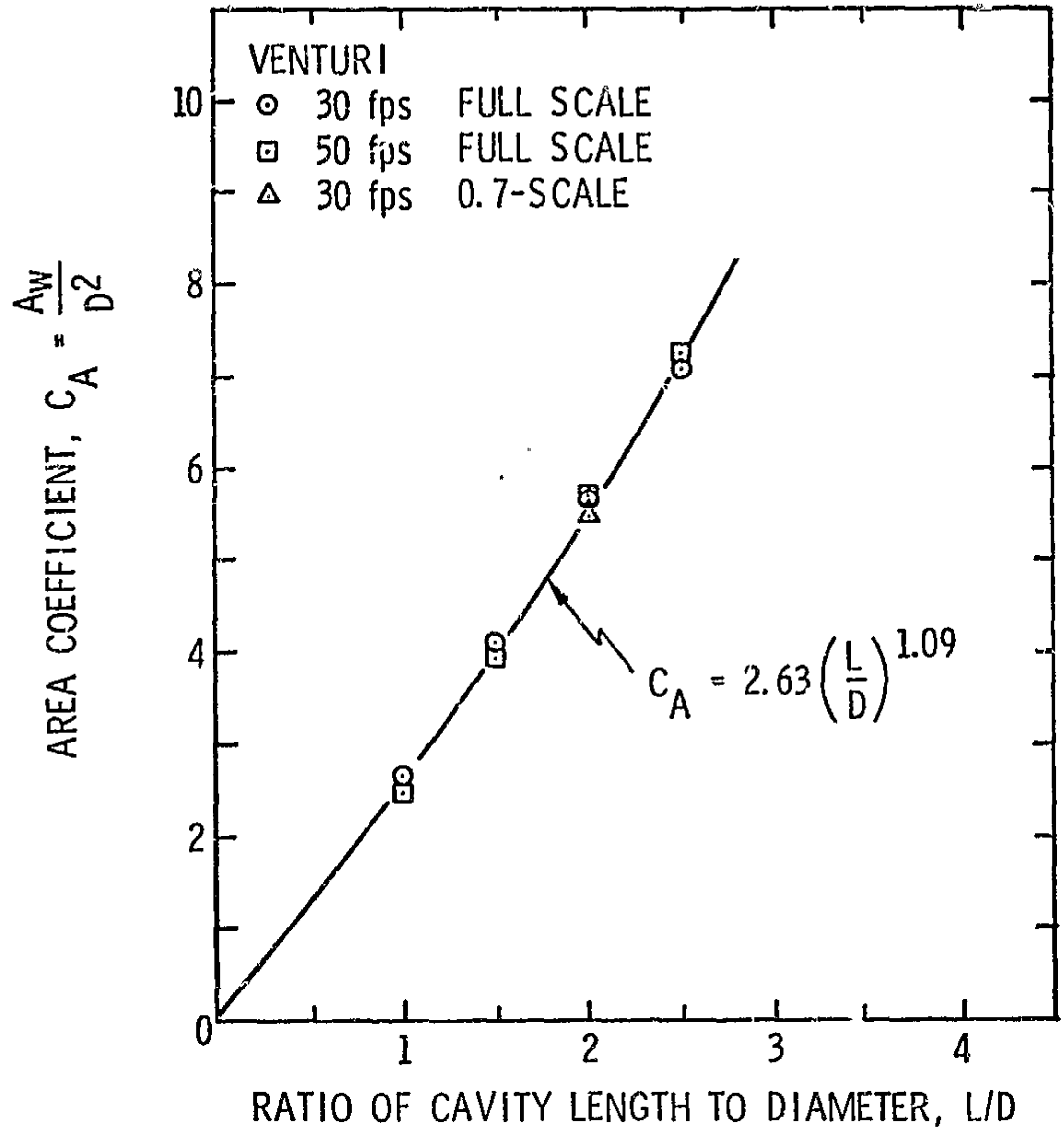

Figure 9 - Area Coefficient for the Venturis

December 11, 1975
MLB:JWH:DSW:jep

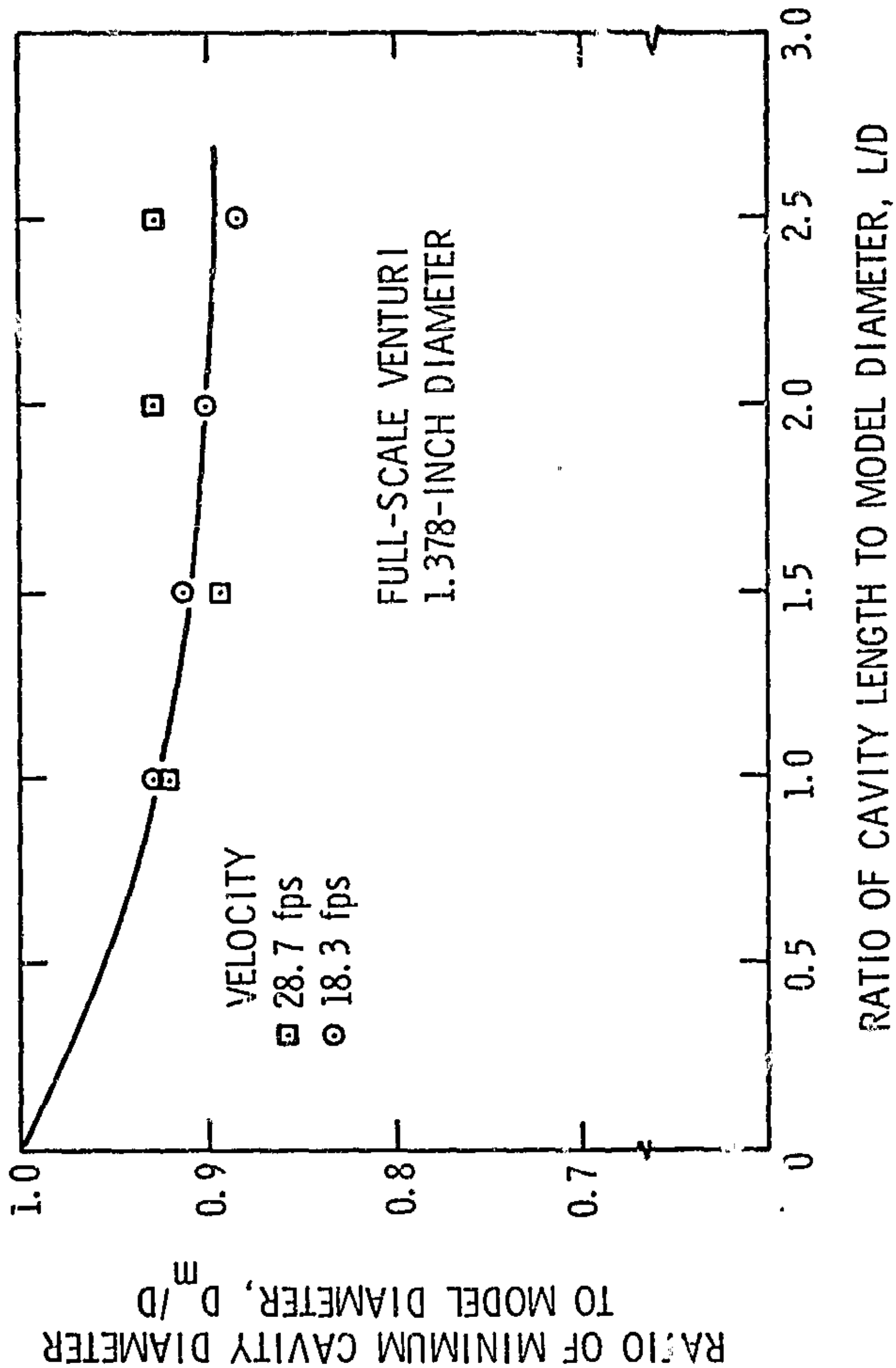

Figure 10 - Dimensionless Minimum Cavity Diameter for the Venturis

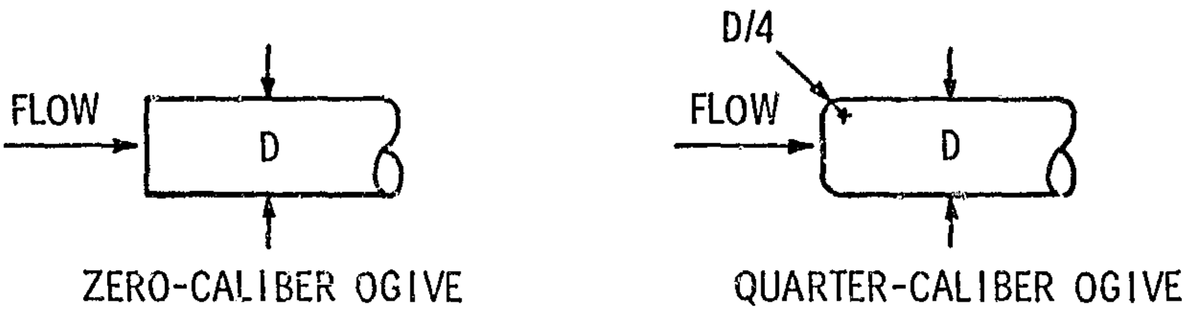

OGIVE TEST CONDITIONS FOR ΔT TESTS

MODEL DIAMETER (D): 0.125 AND 0.250 INCH

DIMENSIONLESS CAVITY LENGTH (L/D): 1.0 TO 7.0

VELOCITY RANGE: 64 ft/sec TO 120 ft/sec

TEMPERATURE RANGE: 85°F TO 203°F IN FREON 113
140°F TO 260°F IN WATER

Figure 11 - Sketch of the Ogives and Description of Test Conditions

DISTRIBUTION LIST FOR UNCLASSIFIED TM 75-291
by M. L. Billet, J. W. Holl, and D. S. Weir,
December 11, 1975

Commander
Naval Sea Systems Command
Department of the Navy
Washington, DC 20362
Attn: Library
Code SEA-09G32
(Copy No. 1-2)

Commander
Naval Sea Systems Command
Department of the Navy
Washington, DC 20362
Attn: T. E. Peirce
Code SEA-0351
(Copy No. 3)

Commanding Officer
Naval Underwater Systems Center
Newport, RI 02840
Attn: Library
(Copy No. 4)

Officer-in-Charge
Naval Undersea Center
San Diego Laboratory
San Diego, CA 92132
Attn: Library
(Copy No. 5)

Commander
Naval Surface Weapon Center
Silver Spring, MD 20910
Attn: Library
(Copy No. 6)

Commanding Officer & Director
David W. Taylor Naval Ship Res. & Dev. Center
Department of the Navy
Bethesda, MD 20084
Attn: Library
(Copy No. 7)

Defense Documentation Center
5010 Duke Street
Cameron Station
Alexandria, VA 22314
(Copy Nos. 8-19)

Dr. Allan J. Acosta
Prof. of Mechanical Engineering
Division of Engineering and
Applied Science
California Institute of Technology
Pasadena, CA 91109
(Copy No. 20)

Mr. Werner R. Britsch
Lewis Research Center
National Aeronautics and Space
Administration
Mail Stop 5-9
21000 Brookpark Road
Cleveland, OH 44135
(Copy Nos. 21-23)

Mr. M. J. Hartman
Lewis Research Center
National Aeronautics and Space
Administration
Mail Stop 5-9
21000 Brookpark Road
Cleveland, OH 44135
(Copy No. 24)

Hydronautics, Inc.
Pindell School Road
Laurel, MD 20810
Attn: Library
(Copy No. 25)

Mr. T. Gelder
Lewis Research Center
National Aeronautics and Space
Administration
Mail Stop 5-9
21000 Brookpark Road
Cleveland, OH 44135
(Copy No. 26)

Mr. R. Ruggeri
Lewis Research Center
National Aeronautics and Space
Administration
Mail Stop 5-9
21000 Brookpark Road
Cleveland, OH 44135
(Copy No. 27)

Mr. L. Gross
R-P and VE
Marshall Space Flight Center
Huntsville, Alabama
(Copy No. 28)

Mr. A. F. Lehman
Head, Water Tunnel Division
Oceanics, Inc.
Technical Industrial Park
Plainview, Long Island
New York 11803
(Copy No. 29)

Mr. Robert Waid
Lockheed Aircraft Corp.
Division No. 81-73, Bldg. 538
Post Office Box 504
Sunnyvale, CA 94088
(Copy No. 30)

Dr. J. W. Holl
The Pennsylvania State University
Institute for Science & Engineering
Applied Research Laboratory
Post Office Box 30
State College, PA 16801
(Copy Nos. 31-35)

Mr. Michael L. Billet
The Pennsylvania State University
Institute for Science & Engineering
Applied Research Laboratory
Post Office Box 30
State College, PA 16801
(Copy No. 36)

2Lt. Donald Weir
5418 D Gilkey St.
Fort Knox, Kentucky 40121
(Copy No. 37)

Garfield Thomas Water Tunnel Library
The Pennsylvania State University
Institute for Science & Engineering
Applied Research Laboratory
Post Office Box 30
State College, PA 16801
(Copy No. 38)

NASA Scientific and Technical Information Faciltiy
P. O. Box 8757
Baltimore/Washington International Airport
Baltimore, MD 21240
(Copy Nos. 39-43)

Dr. P. Leehey
Department of Naval Architecture & Marine Engineering
Massachusetts Institute of Technology
Cambridge, Massachusetts 02139
(Copy No. 44)

Dr. C D. Lovstad
The Norwegian Ship Model Experiment Tand
Trondheim
Norway
(Copy No. 45)

Dr. Hans Lindgren
Statens Skeppsprovningsanstalt
Box 24001
Goteborg 24
Sweden
(Copy No. 46)

Mr. J. H. J. van der Meulen
Netherlandsch Scheepsbouwkundig Proefstation
Haagsteeg 2
Post Box 28
Wageningen
Holland
(Copy No. 47)

Dr. I. S. Pearsall
Department of Scientific & Industrial Research
National Engineering Laboratory
East Kilbride
Glasgow, Scotland
(Copy No. 48)

Dr. John W. English
National Physical Laboratory
Teddington, Middlesex
England
(Copy No. 49)

Dr. Albert T. Ellis
University of California
Department of Applied Mechanics
La Jolla, CA 92038
(Copy No. 50)

Dr. F. G. Hammit
Professor of Mechanical Engineering
The University of Michigan
Ann Arbor, Michigan 48105
(Copy No. 51)

Dr. J. F. Kennedy
Iowa Institute of Hydraulic Research
State University of Iowa
Iowa City, Iowa 52240
(Copy No. 52)

St. Anthony Falls Hydraulic Laboratory
Institute of Technology
University of Minnesota
Mississippi River at 3rd Avenue, S.E.
Minneapolis, Minnesota 55414
Attn: Library
(Copy No. 53)

Dr. J. M. Robertson
125 Talbot Laboratory
University of Illinois
Urbana, Illinois 61801
(Copy No. 54)

Dr. A. Thiruvengadam
Mechanical Engineering Department
The Catholic University of America
Washington, DC 20017
(Copy No. 55)

Dr. D. R. F. Harleman
Hydrodynamics Laboratory
Massachusetts Institute of Technology
Cambridge, Massachusetts 02139
(Copy No. 56)

Prof. J. Bonnin
Electricite de France
Direction Des Etudes et Recherches
6 Quai Watier 78 Chatou
France
(Copy No. 57)

Institute of High Speed Mechanics
Tohoku University
Sendai, Japan
Attn: Library
(Copy No. 58)

Prof. J. C. Raabe
Direktor des Instituts fur hydr.
Maschinen und Analagen
Technischen Hochschule
Munchen
Arcisstrasse 21, 8 Munchen 2
Germany
(Copy No. 59)

Dr. Claus Kruppa
Institut fur Scheffstechnik
Technische Universitat Berlin
Salzufer 17 - 19
1 Berlin 10 (Charlottenburg)
West Germany
(Copy No. 60)

Prof. S. P. Hutton
Department of Mechanical Engineering
The University
Southampton, S09, 5 NH
England
(Copy No. 61)

Mr. Jesse Hord
Cryogenic Engineering Laboratory
U. S. Department of Commerce
National Bureau of Standards
Boulder Laboratories
Boulder, Colorado
(Copy No. 62)

Dr. A. P. Keller
Lehrstuhl fur Wasserbau und
Wasserwirtschaft
Versuchsanstalt fur Wasserbau
Technische Universitat Munchen
Oskar v. Miller-Institut
D 811 Obernach
Post Walchensee
West Germany
(Copy No. 63)

Dr. E. Reshotko
Case Western Reserve University
10900 Euclid Ave.
Cleveland, OH 44106
(Copy No. 64)

Dr. Paul Cooper
Engineering Specialist
TRW Accessories Division
2448 Euclid Heights Blvd.
Cleveland, OH 44106
(Copy No. 65)

Onera Library
Office National D'Etudes et de
Recherches Aerospatiales
29 Avenue de la Division Leclerc
Chatillon-sous-Bagneux (Hauts
de Seine)
France
(Copy No. 66)

Oxford University
Oxford, England
Attn: Library
(Copy No. 67)

Cambridge Univeristy
Cambridge, England
Attn: Library
(Copy No. 68)

Rocketdyne Division
North American Aviation
6633 Canoga Avenue
Canoga Park, CA 91303
Attn: Library
(Copy No. 69)

Aerojet General
Post Office Box 15847
Sacramento, CA 15813
Attn: Library
(Copy No. 70)

Dr. Rothe
Department 596-115
Rocketdyne Division
North American Aviation
6633 Canoga Avenue
Canoga Park, CA 91303
(Copy No. 71)

Dr. Jackobsen
Rocketdyne Division
North American Aviation
6633 Canoga Avenue
Canoga Park, CA 91303
(Copy No. 72)

Dr. Robert Y. Ting
Code 6170
Naval Research Laboratory
Washington, DC 20375
(Copy No. 73)

Mr. M. E. P. Wykes
Research Engineer
University of Oxford
Department of Engineering Science
Parks Road
Oxford OX13PJ England
(Copy No. 74)